N-acyl taurines are endogenous lipid messengers that improve glucose homeostasis

Trisha J. Grevengoed[a], Samuel A. J. Trammell[a], Michele K. McKinney[b,c], Natalia Petersen[a], Rebecca L. Cardone[d], Jens S. Svenningsen[a], Daisuke Ogasawara[b,c], Christina C. Nexøe-Larsen[e], Filip K. Knop[a,e,f,g], Thue W. Schwartz[a], Richard G. Kibbey[d], Benjamin F. Cravatt[b,c,1], and Matthew P. Gillum[a,1]

[a]Novo Nordisk Foundation Center for Basic Metabolic Research, Faculty of Health and Medical Sciences, University of Copenhagen, 2200 Copenhagen, Denmark; [b]Department of Cell Biology, The Scripps Research Institute, La Jolla, CA 92037; [c]Department of Chemistry, The Scripps Research Institute, La Jolla, CA 92037; [d]Department of Internal Medicine, Yale School of Medicine, New Haven, CT 06519; [e]Center for Clinical Metabolic Research, Gentofte Hospital, University of Copenhagen, 2900 Hellerup, Denmark; [f]Department of Clinical Medicine, Faculty of Health and Medical Sciences, University of Copenhagen, 2200 Copenhagen, Denmark; and [g]Clinical Metabolic Physiology, Steno Diabetes Center Copenhagen, Gentofte, 2820 Hellerup, Denmark

Contributed by Benjamin F. Cravatt, October 17, 2019 (sent for review September 19, 2019; reviewed by George Kunos and Richard Lehner)

Fatty acid amide hydrolase (FAAH) degrades 2 major classes of bioactive fatty acid amides, the *N*-acylethanolamines (NAEs) and *N*-acyl taurines (NATs), in central and peripheral tissues. A functional polymorphism in the human *FAAH* gene is linked to obesity and mice lacking FAAH show altered metabolic states, but whether these phenotypes are caused by elevations in NAEs or NATs is unknown. To overcome the problem of concurrent elevation of NAEs and NATs caused by genetic or pharmacological disruption of FAAH in vivo, we developed an engineered mouse model harboring a single-amino acid substitution in FAAH (S268D) that selectively disrupts NAT, but not NAE, hydrolytic activity. The FAAH-S268D mice accordingly show substantial elevations in NATs without alterations in NAE content, a unique metabolic profile that correlates with heightened insulin sensitivity and GLP-1 secretion. We also show that *N*-oleoyl taurine (C18:1 NAT), the most abundant NAT in human plasma, decreases food intake, improves glucose tolerance, and stimulates GPR119-dependent GLP-1 and glucagon secretion in mice. Together, these data suggest that NATs act as a class of lipid messengers that improve postprandial glucose regulation and may have potential as investigational metabolites to modify metabolic disease.

N-acyl taurines | fatty acid amide hydrolase | metabolism | lipid signaling

Fatty acid amide hydrolase (FAAH) degrades 2 major classes of lipid metabolites, the *N*-acylethanolamines (NAEs) and *N*-acyl taurines (NATs), which act as signaling molecules in the central nervous system and peripheral tissues (1, 2). Single-nucleotide polymorphisms (SNPs) linked to reduced FAAH expression are associated with human obesity, suggesting that an accumulation of its lipid substrates may impact energy balance (3, 4). One relevant and well-studied substrate is the endocannabinoid *N*-arachidonoylethanolamine (AEA; anandamide) (5), which suppresses pain and anxiety while increasing appetite and impairing glucose tolerance via cannabinoid receptor 1 (CB1) (6, 7). Other FAAH-catabolized NAEs, such as *N*-oleoylethanolamine (OEA), in contrast, have beneficial metabolic effects, reducing food intake (8, 9) and increasing glucagon-like peptide 1 (GLP-1) secretion via GPR119, an abundant receptor in pancreatic and intestinal endocrine cell populations (10, 11).

FAAH knockout (FAAH-KO) mice and selective FAAH inhibitors have been used to study the function of this enzyme and its endogenous lipid substrates (12) and, in cases where organismal phenotypes can be blocked by CB1 and/or CB2 antagonists (13–17), assignment of AEA as a contributory lipid can be made with confidence. However, the concurrent elevation of NAEs and NATs in FAAH-inactivated animals complicates the mechanistic interpretation of CB1/2-independent phenotypes (1). Metabolically, these mice are susceptible to obesity, fatty liver, and insulin resistance—phenotypes that have been attributed to an accumulation of NAEs that include but may extend beyond the endocannabinoid AEA (7, 18, 19). The focus on NAEs due to their involvement in the endocannabinoid system may have, to date, overshadowed the study of NATs, the physiological functions of which remain poorly understood despite their bioactivity and dysregulation in disease states (20–22).

NATs have been identified by liquid chromatography-tandem mass spectrometry (LC-MS/MS) in both rodent (1) and human (21) tissue, and putative mediators of NAT synthesis have been described. Hepatic peroxisomal acyl-CoA:amino acid *N*-acyltransferase 1 and bile acid-CoA:amino acid *N*-acyltransferase can synthesize NATs in vitro (23, 24). NATs undergo high turnover in tissues that regulate systemic metabolism, with certain acyl species increasing more than 100-fold in the liver following acute pharmacological FAAH inhibition (2). Recently, untargeted MALDI-MS metabolomics revealed that NAT levels are elevated in pancreatic islets from diabetic humans and mice and stimulate insulin secretion in isolated murine islets and cell lines (21, 25). However, whether NATs regulate metabolic homeostasis has not been evaluated in vivo.

Here we hypothesized that NATs contribute to the insulin-resistant phenotype found in FAAH-disrupted mice. We tested this hypothesis by developing an innovative genetic mouse model

Significance

Deletion of fatty acid amide hydrolase (FAAH) in mice results in the concomitant elevation of 2 major types of fatty acid amides, *N*-acylethanolamines (NAEs) and *N*-acyl taurines (NATs), as well as obesity, hyperphagia, and insulin resistance. However, the respective contribution of each class of fatty acid amide to these phenotypes is unresolved. Here we employ an engineered variant of FAAH to specifically elevate NATs in vivo and administer the predominant circulating human NAT species to mice, demonstrating that NATs improve insulin sensitivity and augment secretion of the antidiabetic hormone GLP-1. These findings expose a divergent role for FAAH substrates in the regulation of glucose homeostasis, informing future efforts to target fatty acid amide signaling to treat metabolic disease.

Author contributions: T.J.G., S.A.J.T., M.K.M., N.P., R.L.C., J.S.S., D.O., C.C.N.-L., F.K.K., T.W.S., R.G.K., B.F.C., and M.P.G. designed research; T.J.G., S.A.J.T., M.K.M., N.P., R.L.C., J.S.S., D.O., C.C.N.-L., F.K.K., T.W.S., and R.G.K. performed research; T.J.G., S.A.J.T., M.K.M., N.P., R.L.C., J.S.S., D.O., C.C.N.-L., F.K.K., T.W.S., and R.G.K. contributed new reagents/analytic tools; T.J.G., S.A.J.T., M.K.M., N.P., R.L.C., J.S.S., D.O., C.C.N.-L., F.K.K., T.W.S., R.G.K., B.F.C., and M.P.G. analyzed data; and T.J.G., B.F.C., and M.P.G. wrote the paper.

Reviewers: G.K., National Institutes of Health; and R.L., University of Alberta.

The authors declare no competing interest.

[1]To whom correspondence may be addressed. Email: cravatt@scripps.edu or gillum@sund.ku.dk.

This article contains supporting information online at https://www.pnas.org/lookup/suppl/doi:10.1073/pnas.1916288116/-/DCSupplemental.

First published November 18, 2019.

expressing a FAAH variant with impaired NAT but not NAE hydrolytic activity. This animal model shows selective elevations in NATs while maintaining normal NAE content, a heretofore unstudied metabolic profile that we find surprisingly correlates with improved insulin sensitivity and GLP-1 secretion, thereby contrasting with the insulin-resistant phenotype observed in conventional FAAH-KO mice that have increases in both NATs and NAEs. We further identify *N*-oleoyl taurine (C18:1 NAT) as the most abundant NAT in human plasma and show that this lipid acts as an agonist for GPR119, leading to higher GLP-1 in circulation and improved glucose tolerance following acute administration to mice. This work describes an animal model for studying the specific functions of NATs in vivo and shows a beneficial role for these lipid transmitters, distinct from that of NAEs, in the regulation of glucose metabolism.

Results

A Single-Point Mutation in FAAH Inhibits Hydrolytic Metabolism of NATs but Not NAEs In Vivo. FAAH mediates the hydrolysis of multiple classes of amidated lipids, including NAEs and NATs. NAEs are a well-studied class of lipid signaling molecules that can regulate food intake, pain perception, and glucose metabolism (6, 12, 18). NATs are a more recently described set of bioactive lipids (1, 20) and consequently less well characterized in terms of their cellular and physiological functions. Conventional FAAH-KO mice or mice treated with FAAH inhibitors have substantial elevations in both NAEs and NATs (1, 20), which complicates the interpretation of the functional impact of each deregulated class of bioactive lipids. To overcome this problem, we generated a FAAH-knockin mouse with a point mutation that replaces a neutral serine residue in the substrate-binding pocket with a negatively charged aspartate (FAAH-S268D mice; Fig. 1 *A* and *B* and *SI Appendix*, Fig. S1). This S268D mutation corresponds to a G268D mutation previously shown in rat FAAH to selectively impair NAT but not NAE hydrolysis rates, presumably due to the introduction of a charge–charge repulsion with the taurine sulfate group of NATs (26). Consistent with these in vitro substrate selectivity data, NAE content was highly elevated in FAAH-KO liver tissue but not in FAAH-S268D tissue (Fig. 1*C*). On the other hand, both the FAAH-S268D and FAAH-KO mice displayed markedly elevated liver NAT content compared with FAAH-WT (wild-type) mice (Fig. 1*D*). Depending on the specific NAT, the FAAH-S268D mice either showed equivalent or partial elevations compared with FAAH-KO mice (Fig. 1*D*), which might reflect differing degrees of impairment of hydrolysis of these NATs by the S268D mutant enzyme. Brain tissue from FAAH-S268D mice also showed selective elevations in NATs but not NAEs, although the increases in NATs did not reach the same magnitude as those observed in FAAH-KO mice (*SI Appendix*, Fig. S1). Consistent with the high liver NAT content, FAAH-S268D mice showed elevated plasma NATs compared with FAAH-WT mice (Fig. 1*E*) and also showed impaired ability to degrade exogenously administered C18:1 NAT compared with FAAH-WT mice (Fig. 1*F*). These data, taken together, indicate that the FAAH-S268D knockin mouse provides an in vivo model system for studying elevated NATs against a background of unperturbed NAE content.

Chronic Elevation of Endogenous NATs Improves Insulin Sensitivity and GLP-1 Secretion. Chow-fed FAAH-S268D mice displayed lower blood glucose following a low-dose insulin tolerance test (Fig. 2*A*) and increased glucagon secretion 1.8-fold more than controls 30 min after insulin injection (Fig. 2*B*) compared with FAAH-WT mice, indicating that a deficiency in glucagon secretion did not cause the increased insulin sensitivity. Oral glucose tolerance was not different between genotypes (Fig. 2*C*), although FAAH-S268D mice displayed postglucose plasma insulin concentrations that were substantially lower than FAAH-WT mice (Fig. 2*D*), consistent with improved insulin sensitivity. In FAAH-S268D mice fed a mixed meal, GLP-1 secretion tended to be higher after 10 min ($P = 0.076$) and was 2.1-fold higher after 30 min (Fig. 2*E*). Gastric inhibitory peptide (GIP) and insulin levels were not altered (Fig. 2 *F* and *G*).

FAAH-KO mice are hyperphagic (19), and mice expressing a different FAAH SNP (C385A), which leads to a reduction in FAAH activity, do not decrease food intake in response to leptin (27). To determine if chronic elevation of endogenous NATs contributed to altered food intake or leptin insensitivity, chow consumption was monitored before and after leptin treatment. The chronic elevation of endogenous NATs in FAAH-S268D mice did not alter food intake compared with FAAH-WT mice (Fig. 2*H*). Additionally, leptin treatment lowered food intake in FAAH-S268D mice (Fig. 2*H*), indicating that elevated NATs may improve leptin resistance and that the leptin-resistant phenotype seen with partial or complete loss of FAAH may be due to elevation of NAEs. This latter finding is consistent with the leptin-sensitizing effects of CB1 inverse agonists (28), which block AEA (C20:4 NAE), but not NAT, signaling.

Acute Treatment with Exogenous C18:1 NAT Improves Glucose Tolerance and GLP-1 Secretion. We next quantified NATs in human plasma using LC-MS and found that C18:1 NAT was present at the highest circulating concentrations (Fig. 3*A*). Because of its abundance and shared acyl chain with OEA, an NAE that can regulate GLP-1 secretion (10), we focused on characterizing the pharmacological effects of C18:1 NAT on glucose homeostasis. In C57BL/6N mice, pharmacokinetic experiments demonstrated that C18:1 NAT was removed from the blood within 30 min of injection (Fig. 3*B*), indicating rapid hydrolysis or clearance into other body compartments. High-fat, high-sucrose (HFHS) diet-fed mice displayed improved glucose tolerance 15 min after a single dose of 10 mg/kg C18:1 NAT, lowering peak glucose by 22% compared with control mice treated with a mixture of unconjugated oleic acid and taurine (FA+Tau) (Fig. 3*C*), indicating C18:1 NAT is responsible for the activity rather than its chemical components. With a mixed meal, C18:1 NAT treatment increased GLP-1 and glucagon levels 2.9- and 1.8-fold, respectively, over controls (Fig. 3*D*). Insulin trended higher after C18:1 NAT treatment ($P = 0.073$). Therefore, acute treatment with C18:1 NAT has the potential to improve blood glucose control.

Acute Treatment with C18:1 NAT Decreases Food Intake. The structurally related FAAH substrate OEA decreases food intake in mice (8, 9). We hypothesized C18:1 NAT may serve a similar role, so we next evaluated the impact of C18:1 NAT on appetite. C57BL/6N male mice treated once per day with 10 mg/kg C18:1 NAT decreased food intake by 17%, whereas control mice did not change food intake with FA+Tau treatment (Fig. 4*A*). The difference in food intake persisted 24 h after treatment (Fig. 4*B*), despite the rapid clearance of plasma C18:1 NAT (Fig. 3*B*), indicating C18:1 NAT initiated a signaling pathway that affected food intake long after the disappearance of this lipid from plasma. C18:1 NAT-mediated change in food intake was reversible, normalizing over the 4-d washout period (Fig. 4*C*). FA+Tau–treated mice did not lose weight, whereas mice treated with C18:1 NAT lost 0.4 g (1.6% of total body weight; BW) during the 3-d treatment period (Fig. 4*D*). C18:1 NAT treatment decreased the number of meals eaten per day without changing the meal size (Fig. 4 *E* and *F*), indicating less hunger between meals and a potential activity of C18:1 NAT as an appetite suppressant.

GPR119 Is Required for C18:1 NAT-Stimulated GLP-1 Secretion in Intestinal Organoids. Because single-dose C18:1 NAT rapidly improved glucose tolerance, we hypothesized that NATs might signal through a specific receptor(s) to stimulate glucoregulatory hormone secretion. Therefore, we screened the ability of C18:1

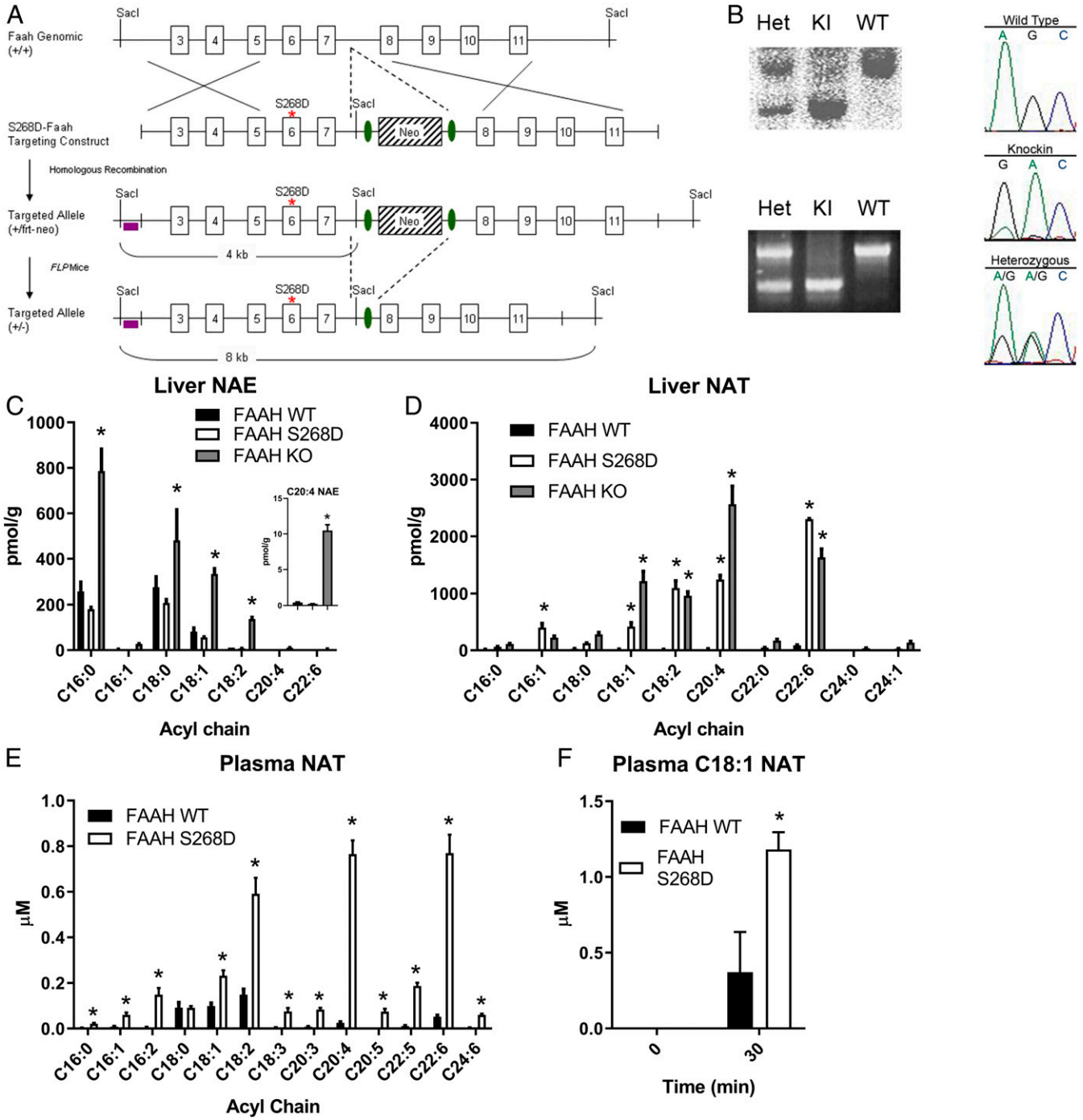

Fig. 1. Single-point mutation in FAAH inhibits hydrolytic metabolism of NATs but not NAEs in vivo. (*A*) Schematic for generation of FAAH-S268D knockin mice. (*B*) Confirmation of FAAH-S268D mutation by Southern blotting, PCR, and genome sequencing. (*C* and *D*) NAEs (*C*) and NATs (*D*) in liver of FAAH-WT control, FAAH-S268D, and FAAH-KO mice ($n = 3$ or 4 per group). (*C*, *Inset*) C20:4 NAE (AEA). (*E*) NATs in plasma from FAAH-WT control and FAAH-S268D mice ($n = 10$ or 11 per group). (*F*) Plasma C18:1 NAT levels 30 min after injection of C18:1 NAT ($n = 3$). Data are presented as mean ± SEM. $^*P < 0.05$ compared with control.

NAT to activate a range of candidate G protein-coupled receptors (GPCRs) enriched in endocrine cells of the gut and pancreas. C18:1 NAT activated human and murine GPR119 at concentrations similar to the endogenous GPR119 agonist OEA, whereas other known fatty acid-activated GPCRs (GPR40A, GPR41, GPR43, GPR84, and GPR120) were not stimulated by C18:1 NAT (Fig. 5*A* and *SI Appendix*, Fig. S2).

GLP-1 secretion with C18:1 NAT stimulation was evaluated in organoids generated from duodenum, ileum, and colon of GPR119-KO mice and littermate GPR119-WT mice. In the duodenum, 100 µM C18:1 NAT stimulated a modest increase in GLP-1 secretion (Fig. 5*B*). In both the ileum and colon, which contain higher proportions of GLP-1–secreting cells than the duodenum (29), C18:1 NAT increased GLP-1 secretion in a dose-dependent manner (Fig. 5 *C* and *D*), up to 7-fold over vehicle. Importantly, C18:1 NAT-stimulated GLP-1 secretion was lost in all organoid preparations from GPR119-KO mice, indicating the necessity of GPR119 in mediating the actions of C18:1 NAT.

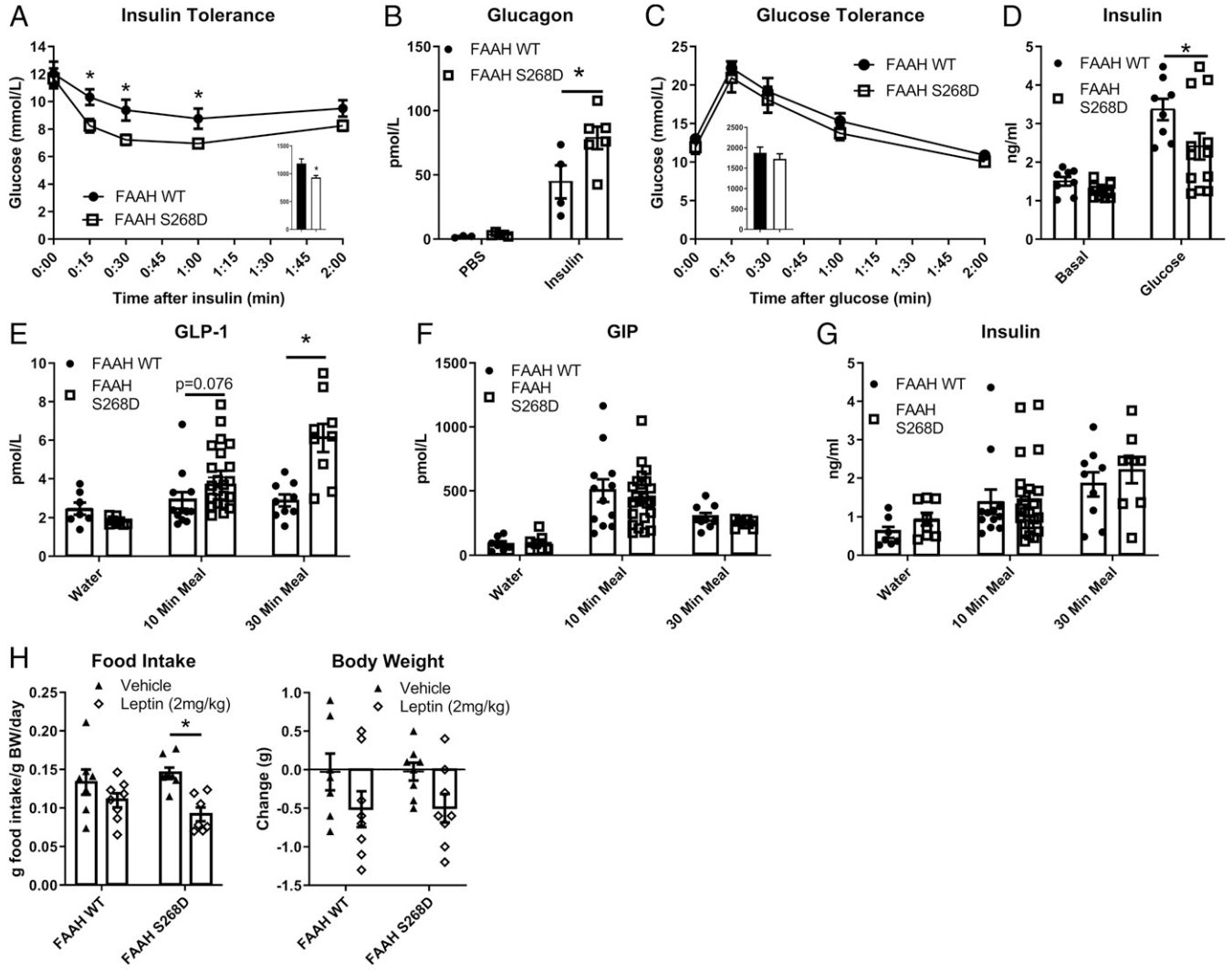

Fig. 2. Chronic elevation of endogenous NATs improves insulin sensitivity and GLP-1 secretion. (*A*) Insulin tolerance test (0.5 U/kg) in lean, 7-wk-old males ($n = 9$ or 10). (*B*) Plasma glucagon 30 min after i.p. PBS or insulin ($n = 3$ to 6). (*C*) Glucose tolerance in lean, 9-wk-old males ($n = 6$ to 8). (*D*) Plasma insulin before and 10 min after oral glucose ($n = 8$ to 12). (*E–G*) Hormone secretion after oral water or mixed meal ($n = 7$ to 22). (*H*) Twenty-four-hour food intake and body weight change after leptin or vehicle (PBS) ($n = 7$ or 8). Data are presented as mean ± SEM. *$P < 0.05$ between genotypes within treatment.

C18:1 NAT Requires GPR119 to Stimulate Glucagon Secretion. Because GLP-1 regulates both insulin and glucagon secretion in vivo (30), isolated human islet cell reaggregates were treated with 10 μM C18:1 NAT to determine if NATs directly stimulated glucagon and insulin secretion. Human islet cells did not increase insulin secretion in response to C18:1 NAT (Fig. 5*E* and *SI Appendix*, Fig. S3) but instead secreted 23% more glucagon with greater increases at low glucose concentrations (Fig. 5*F* and *SI Appendix*, Fig. S3), indicating that C18:1 NAT had a selective effect on human alpha cells.

At 10 μM, C18:1 NAT did not stimulate insulin secretion from pancreatic islets isolated from either GPR119-WT or GPR119-KO mice (Fig. 5*G*). However, C18:1 NAT promoted substantial glucagon secretion from GPR119-WT but not GPR119-KO islets (Fig. 5*H*), indicating that GPR119 is required for direct stimulation of alpha-cell glucagon secretion by C18:1 NAT. Taken together, the islet studies indicate that C18:1 NAT is able to directly stimulate glucagon secretion but any increased insulin secretion seen in vivo is likely due to higher GLP-1 concentrations.

GPR119 Is Required for C18:1 NAT-Mediated Improvement in Glucose Tolerance but Not Food Intake. To test if NATs signal through GPR119 in vivo, we measured the effects of C18:1 NAT on glucoregulatory hormone secretion in mice lacking GPR119. In contrast to GPR119-WT mice, GPR119-KO mice treated with C18:1 NAT showed no improvement in glucose tolerance compared with treatment with FA+Tau (Fig. 6*A*). After a mixed meal, GPR119-KO mice given FA+Tau showed normal levels of GLP-1, GIP, insulin, and glucagon in blood, whereas C18:1 NAT treatment increased GLP-1, GIP, and insulin secretion in GPR119-WT but not GPR119-KO mice (Fig. 6 *B–E*). Interestingly, C18:1 NAT treatment lowered GLP-1 secretion in GPR119-KO mice, potentially indicating that in the absence of GPR119, C18:1 NAT could inhibit GLP-1 secretion and impair glucose tolerance. These findings indicate GPR119 is necessary for C18:1 NAT to stimulate glucoregulatory hormone secretion in vivo. In contrast to the glucose regulatory findings, loss of GPR119 did not alter C18:1 NAT-mediated reductions in food intake (Fig. 6*F*), indicating that this behavior is controlled by an alternate pathway.

GPR119 Is Required for Elevated GLP-1 Secretion in FAAH-S268D Mice. To determine if GPR119 is required for the improved insulin tolerance and GLP-1 secretion seen in FAAH-S268D mice, GPR119-KO mice were crossed with the FAAH-S268D line.

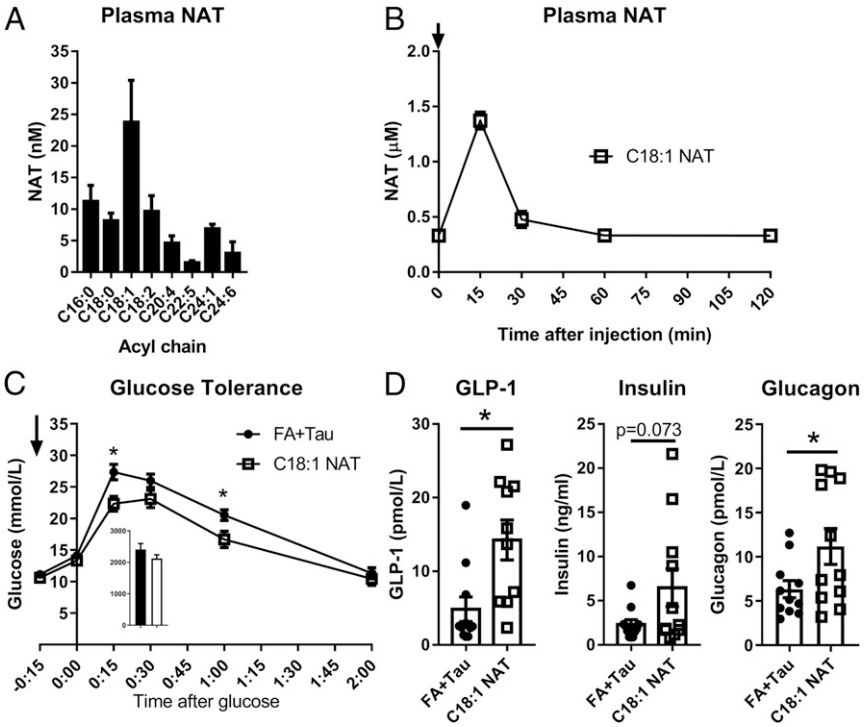

Fig. 3. Acute treatment with exogenous C18:1 NAT improves glucose tolerance and GLP-1 secretion. (*A*) NAT profile of human plasma ($n = 4$). (*B*) Plasma C18:1 NAT after i.v. injection with 10 mg/kg C18:1 NAT ($n = 3$ per time point). (*C*) Glucose tolerance test 15 min after a single dose of 10 mg/kg C18:1 NAT or equimolar dose of oleate and taurine (FA+Tau) in HFHS diet-fed mice ($n = 8$). Arrows indicate time of treatment. (*D*) Plasma GLP-1, insulin, and glucagon after a mixed-meal challenge in HFHS diet-fed mice given a single dose of 10 mg/kg C18:1 NAT or FA+Tau ($n = 10$ to 12). Data are presented as mean ± SEM. $^*P < 0.05$ between treatments.

FAAH-S268D x GPR119-KO (S268D-119KO) mice displayed similar insulin tolerance to littermate FAAH-S268D mice (Fig. 6*G*). GPR119-KO mice tend to be more insulin-sensitive and glucose-tolerant than controls (31) (Fig. 6*A*), potentially due to lack of alpha-cell stimulation without GPR119 leading to diminished glucagon secretion (32, 33). This prevented us from

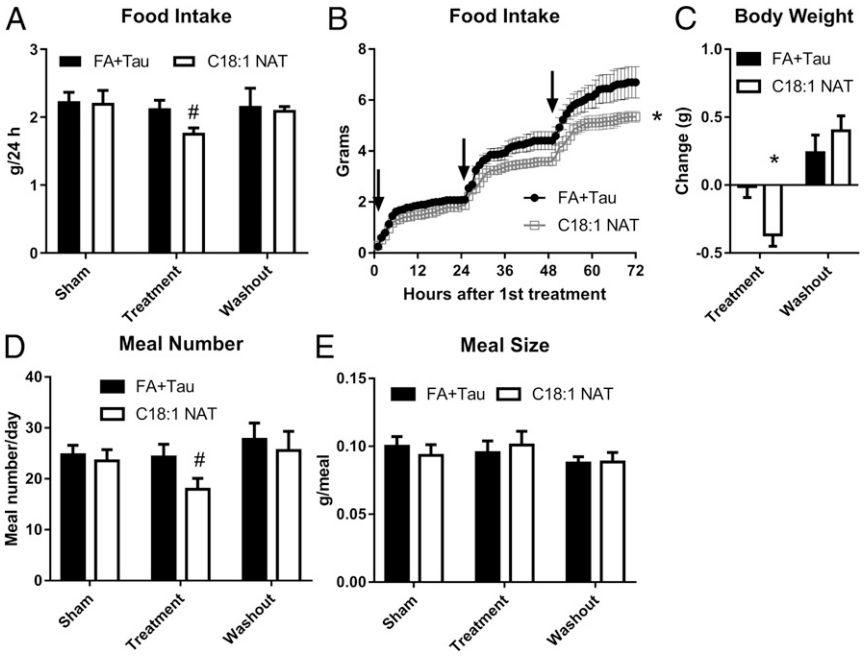

Fig. 4. Acute treatment with C18:1 NAT decreases food intake. Male, 9-wk-old C57BL/6N mice were group-housed and given free access to HFHS diet over a 3-d sham period (anesthesia alone), 3-d treatment with i.v. 10 mg/kg C18:1 NAT or FA+Tau, and 4-d washout ($n = 6$ or 7). (*A*) Average 24-h food intake. (*B*) Cumulative food intake during treatment period. Arrows indicate time of treatment. (*C*) Weight change between study arms. (*D*) Average number of meals over 24 h. (*E*) Average meal size over 24 h. Data are presented as mean ± SEM. $^*P < 0.05$ between treatments within study arm. $^{\#}P < 0.05$ between treatments and sham within group.

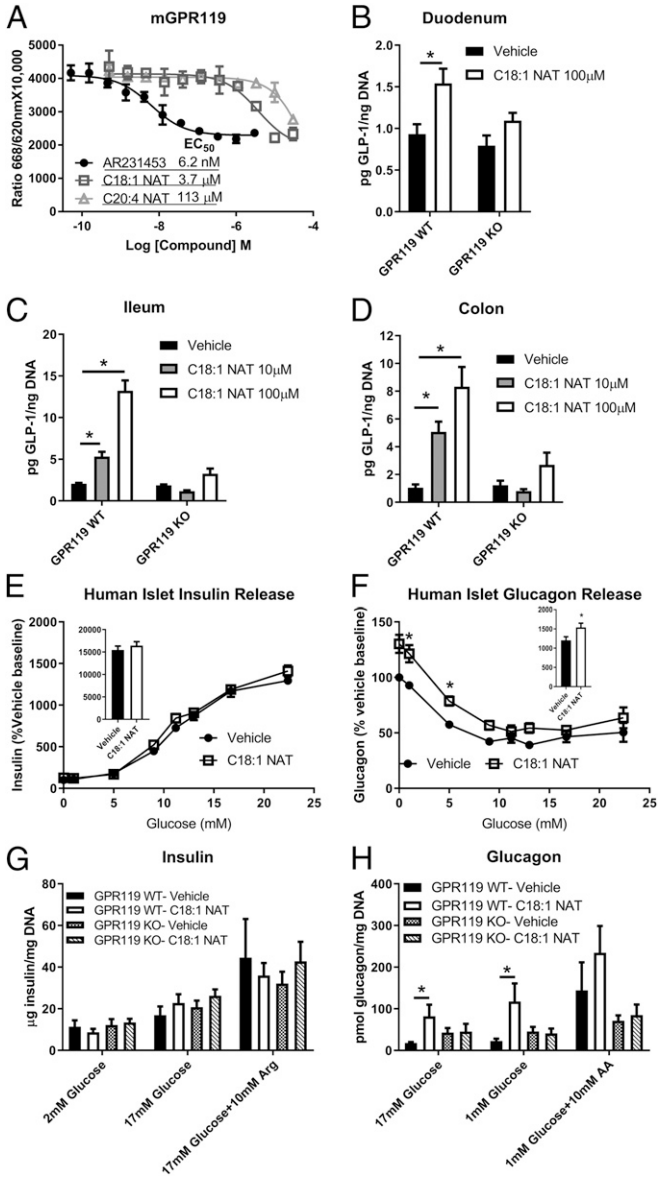

Fig. 5. GPR119 is required for C18:1 NAT-stimulated GLP-1 and glucagon secretion. (*A*) cAMP synthesis assay in CHO cells stably transfected with mouse GPR119; AR231453, synthetic GPR119 agonist (representative curve, in triplicate). Estimated EC_{50} is shown. (*B–D*) GLP-1 secretion from organoids generated from duodenum, ileum, and colon from GPR119-KO mice or littermate GPR119-WT ($n = 3$ separate experiments with 2 to 4 replicates). (*E* and *F*) Insulin and glucagon release from isolated human pancreatic islet cells with 10 μM C18:1 NAT or vehicle (DMSO) (2 nondiabetic patients, in quadruplicate). (*E* and *F*, *Insets*) Area under the curve. (*G* and *H*) Insulin and glucagon secretion in isolated murine pancreatic islets (3 to 5 experiments in triplicate) at the indicated glucose concentration and arginine (Arg) or amino acid mixture (AA). Data are presented as mean ± SEM. $*P < 0.05$.

determining whether GPR119 is necessary for NAT-induced insulin sensitivity. GPR119 was, however, required for acute NAT stimulation of GLP-1 secretion (Fig. 6*B*), allowing us to determine if GPR119 is also required for higher GLP-1 secretion in FAAH-S268D mice with chronically elevated endogenous NATs. When given a mixed meal, S268D-119KO mice had lower blood GLP-1 than FAAH-S268D littermates (Fig. 6*H*), indicating that NAT-stimulated GLP-1 secretion requires GPR119 in both chronic and acute models of elevated NATs.

Discussion

Fatty acids have historically been considered to act as energy storage or structural components of membranes; however, lipids also have clear roles as signaling molecules. Recently, several endogenous fatty acid-based metabolites have been shown to exert endocrine effects on metabolic homeostasis. For instance, palmitic acid hydroxystearic acids positively correlate with insulin sensitivity, increase GLP-1 and insulin secretion, and activate GPR120 and GPR40 (34, 35). *N*-acyl amino acids, such as *N*-18:1 leucine and *N*-18:1 phenylalanine, increase uncoupled respiration in cells, and *N*-18:1 leucine treatment reduces body weight in mice (36). In addition, bacterially derived acyl amides improve host glucose metabolism through activation of GPR119 (37). Here we identify *N*-acyl taurines as a distinctive class of amphipathic, bioactive lipid with a role in metabolic regulation.

NATs, specifically C18:1 NAT, can promote GLP-1, GIP, insulin, and glucagon secretion through activation of GPR119. A single dose of C18:1 NAT rapidly improved glucose tolerance and GLP-1 secretion in wild-type mice, indicating therapeutic potential for insulin resistance. In our hands, C18:1 NAT did not directly alter insulin secretion in human or mouse islets at a concentration of 10 μM. At higher concentrations, however, C18:1 NAT treatment activates TRPV1 to induce insulin release (20, 21, 25), and high in vivo insulin secretion with C18:1 NAT treatment is likely due to higher incretin concentration (31). GPR119 was required for C18:1 NAT-stimulated glucagon secretion likely reflecting the expression of this GPCR on alpha cells (32, 38), agreeing with recent work showing glucagon secretion is stimulated by GPR119 agonists (33). Both the acute and chronic mouse models for elevated NATs are more insulin-sensitive, indicating that, at least in mice, NATs tip the balance between GPR119-stimulated glucagon and GLP-1 secretion toward improved glucose homeostasis.

In this manuscript, we have also introduced a genetic mouse model for assessing the physiological impact of chronic elevations of NATs with unaltered NAEs. This unique metabolic profile was achieved by replacing FAAH-WT with a point mutant FAAH-S268D that displays selective impairment in NAT hydrolysis (26). Coupling the FAAH-S268D model of chronic NAT elevation with acute treatment of an exogenous NAT allowed us to tease out the effects of NATs versus NAEs. For instance, FAAH-S268D mice displayed increased insulin sensitivity and meal-induced GLP-1 secretion, similar to what was observed for the C18:1 NAT treatment of wild-type mice. This phenotype is in contrast to the phenotypes observed in FAAH-KO mice, which have chronic elevations in both NATs and NAEs and are susceptible to insulin resistance (18). Interestingly, treatment with OEA (8, 10) and C18:1 NAT have similar effects on food intake and GLP-1 secretion, but the chronic elevation of endogenous NAEs and NATs causes a very different phenotype from that of heightened NATs alone. Other NAE effector molecules may contribute to this paradoxical phenotypic outcome, as treatment with AEA and *N*-palmitoylethanolamide reduces energy expenditure (18), possibly contributing to weight gain and insulin resistance. Activation of CB1 by AEA (6, 7) in the FAAH-KO model likely overrides the hypophagic effects of C18:1 NAT, and excess weight gain and hepatic steatosis (18) can supersede the insulin-sensitizing effects of NATs. Treatment with C18:1 NAT lowered food intake whereas chronic elevation of endogenous NATs did not, indicating decreased sensitivity to NATs over time or compensation by alternative appetite pathways to maintain normal food intake. However, when leptin was administered to the FAAH-S268D mice, food intake was reduced, indicating that NATs could sensitize the mice to signals to reduce food intake.

Little is currently known about the in vivo synthesis of NATs, beyond that NAT flux is rapid, with certain species increasing more than 100-fold within 3 h of FAAH inhibition (2). The enzymes that are known to synthesize NATs in vitro are hepatic and located

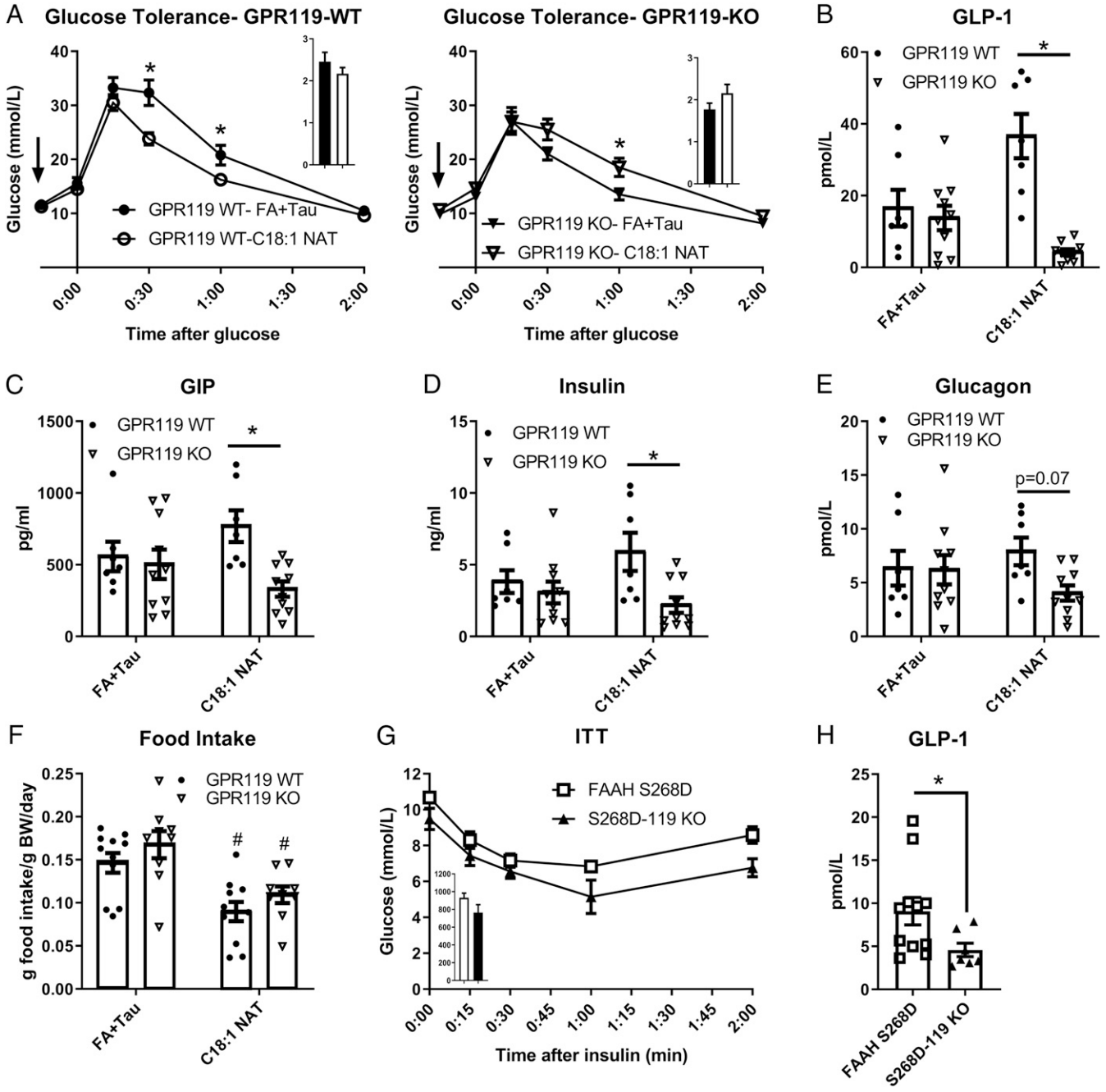

Fig. 6. GPR119 is required for C18:1 NAT-mediated improvement in glucose tolerance but not food intake. (*A*) Glucose tolerance test in littermate GPR119-WT and GPR119-KO male mice after 4 wk of HFHS diet ($n = 7$ to 9). Arrows indicate time of treatment with 10 mg/kg C18:1 NAT or FA+Tau. (*A*, *Insets*) Area under the curve. (*B–E*) Plasma hormone levels after a mixed-meal challenge in HFHS diet-fed mice given a single dose of 10 mg/kg C18:1 NAT or FA+Tau ($n = 7$ to 9). (*F*) Twenty-four-hour food intake (chow) after i.v. 10 mg/kg C18:1 NAT or FA+Tau ($n = 9$ to 11). (*G*) Insulin tolerance test (ITT) in male, chow-fed FAAH-S268D x GPR119-KO (S268D-119KO) and littermate FAAH-S268D mice ($n = 6$ to 9). (*H*) GLP-1 secretion 30 min after a mixed meal ($n = 7$ to 11). Data are presented as mean ± SEM. $^{*}P < 0.05$ between genotypes within treatment; $^{\#}P < 0.05$ between treatments within genotype.

on the peroxisomes (23, 24). We note that the NAT species most highly elevated in the FAAH-S268D mice contain polyunsaturated acyl chains, which may indicate a substrate preference by the synthetic enzyme or an effect of peroxisomal location. These polyunsaturated NAT species could activate different receptors from C18:1 NAT, although C20:4 NAT did not activate any other tested GPCRs (*SI Appendix*, Fig. S1).

Other studies point to the potential relevance of NATs to the pathogenesis of metabolic disorders. NATs are, for instance, elevated in islets from diabetic mice and humans (21), but it is unknown if this relationship is causative, compensatory, or correlative, or which cells produce the NATs. Further studies are required to elucidate if NAT quantity or flux changes with disease in other tissues, such as liver, bile, or plasma. Enhancing endogenous production of NATs or administering specific NATs may be of further value in treating type 2 diabetes and obesity by enhancing secretion of GLP-1, thus improving glucose levels. NATs are stable and readily soluble in water, decreasing the need for complicated vehicles that may have effects on their own. This water solubility may facilitate

NAT access to diverse tissues through circulation as well as to different receptors in or on the cell.

In conclusion, NATs are an endogenous class of bioactive lipids that may contribute to the ontogeny of obesity and type 2 diabetes by regulating glucoregulatory hormone secretion and satiety. Models of both acute and chronic elevation of NATs displayed improved glucose metabolism and increased GPR119-dependent GLP-1 secretion, suggesting opposing effects of NATs and endocannabinoid-related NAEs on energy balance despite their common catabolism by FAAH.

Methods

NAT Synthesis and Quantification. NAEs were measured by LC-MS as described (20). C15:0, C18:0, and C18:1 NATs were synthesized as previously described (22). Human plasma was obtained from 4 female subjects, mean age 54.3 y. The study was approved by the Regional Committee of the Copenhagen Area (Den Videnskabsetiske Komite F for Region Hovedstaden; H-15016324). The subjects gave informed consent prior to any trial activity. Standard quality controls (Std QCs), calibrants, and samples were dosed with an internal standard (C15:0 NAT) prior to extraction. EDTA-produced plasma resting on ice was extracted as described (22) with 2 slight modifications (*SI Appendix, Materials and Methods*). All samples, Std QCs, and calibrants were extracted in the same manner. All samples were suspended in 2-propanol/acetonitrile/water (2:1:1 vol/vol/vol). Equal volumes of all samples were pooled into 1 vial to compose the QC pool. Sample order was randomized prior to analysis.

Samples were separated using chromatography as described (39) with slight modification (*SI Appendix, Materials and Methods*). Analytes ionized via electrospray were detected in full-scan (*m/z* 50 to 1,000), negative-ion mode with a Bruker Impact II Q-TOF.

C18:0 and C18:1 NATs were quantified using an internal standard-normalized calibration curve. Precision and accuracy were measured using quality controls containing either standards alone or standards and human plasma from a separate cohort. All other NATs were identified after peak alignment with XCMS Online (40) based upon intact *m/z* ratio and fragmentation using LC-MS/MS. All comparisons within nontargeted metabolomics were performed using MetaboAnalyst 3.0 (41). Quantities of all NATs other than C18:0 and C18:1 were estimated based upon normalization to the C18:1 NAT concentration multiplied by the C18:1 NAT concentration within the sample. For further details, see *SI Appendix, Materials and Methods*.

Animal Care. Male C57BL/6N mice were obtained from Taconic at 6 to 8 wk of age. FAAH-S268D mice were generated by the B.F.C. laboratory following the general gene-targeting strategy outlined in Fig. 3 and detailed in *SI Appendix, Materials and Methods*. GPR119-KO mice on a C57BL/6N background were obtained from Taconic. All protocols were approved by the Danish Animal Experiments Inspectorate. Mice were housed in a specific pathogen-free environment on a 12-h light/dark cycle. Mice were maintained on regular chow and had free access to food and water unless otherwise specified. For exogenous NAT treatment, C18:1 NAT was solubilized in phosphate-buffered saline (PBS) and injected intravenously (i.v.) at a dose of 10 mg/kg BW. Food intake was measured in the HM-2 System (MBRose) using group-housed, RFID-tagged mice. Mice were acclimated to the chambers and a high-fat, high-sucrose Western diet (Research Diets; D12079B) for 4 d before 3 d of light isoflurane anesthesia (sham), then 3 d of treatment with 10 mg/kg C18:1 NAT or equivalent molarity sodium oleate and taurine (FA+Tau), and then 4 d of washout. For leptin studies, chow-fed mice were given a single dose of 2 mg/kg leptin or PBS vehicle within 1 h of the start of the dark cycle, and food intake was monitored in the HM-2 System.

Glucose and Insulin Tolerance. For dietary studies, glucose tolerance was measured after 4 wk of HFHS feeding. Mice were fasted for 6 h starting 1 to 2 h into the light cycle. For acute NAT treatment, mice were pretreated with 10 mg/kg C18:1 NAT or FA+Tau i.v. 15 min before 2 g/kg glucose. For insulin tolerance, mice were fasted for 4 h starting 2 h into the light cycle. Recombinant human insulin (Sigma; 0.5 IU/kg) was administered via intraperitoneal (i.p.) injection. Blood glucose was monitored using an AlphaTRAK 2 glucometer (Zoetis) via tail nick at −15, 0, 15, 30, 60, and 120 min after injection.

GLP-1, GIP, Glucagon, and Insulin Secretion. For mixed meal-stimulated hormone secretion, mice were fasted for 12 h starting 4 h into the dark cycle. For acute NAT treatment, HFHS-fed male mice were pretreated with 10 mg/kg C18:1 taurine or FA+Tau i.v. before oral gavage of a mixed meal (60% glucose, 20% casein, 20% intralipid [% kcal]). For endogenous NAT studies, chow-fed mice were given the mixed meal via oral gavage. Blood was collected 10 or 30 min after the meal. For hypoglycemic glucagon secretion, blood was collected 30 min after i.p. injection of saline or insulin. For glucose-stimulated insulin secretion, mice were fasted for 6 h and blood was collected before and 10 min after 2 g/kg oral glucose. Total GLP-1 (Mercodia), glucagon (Mercodia), insulin (Mercodia), and total GIP (Millipore) were measured by enzyme-linked immunosorbent assay (ELISA).

G Protein-Coupled Receptor Activation Assays. GPCR activation was measured in Multispan stable cell lines expressing human or mouse GPR119, GPR120, GPR43, GPR40A, GPR41, and GPR84 as previously described (35).

GLP-1 Secretion from Intestinal Organoids. Mouse intestinal organoids were generated from the duodenum, ileum, and colon and cultured as previously described (42, 43). For GLP-1 secretion experiments, an organoid suspension in Matrigel was plated into 96-well plates. After 48 h, organoid cultures were washed 2 times with DMEM/F12 Advanced supplemented with 2 mM L-glutamine and 10 mM Hepes. Then organoids were incubated in the same medium (vehicle) or C18:1 NAT for 2 h at 37 °C. The medium was collected and assayed for total GLP-1 (Meso Scale Discovery) and normalized to the DNA content (DNA Quantitation Kit Fluorescence; Sigma).

Hormone Secretion from Isolated Islets. Human islets from nondiabetic donors were purchased from Prodo Laboratories and dissociated and cultured as previously described (44). Cells were preincubated in standard Krebs–Ringer buffer supplemented with 5 mM glucose, 2 mM glutamine, 24 mM Hepes, and 0.25% BSA for 1.5 h in the presence of 10 μM C18:1 NAT or vehicle (dimethyl sulfoxide; DMSO; 0.1% final) and then incubated for 2 h with the indicated glucose concentration. Insulin (ALPCO) and glucagon (Mercodia) were measured by ELISA.

Murine islets were isolated as previously described (45). Briefly, the pancreas was perfused through the common bile duct with 1 mg/mL collagenase P (Roche). Tissue was digested for 15 min at 37 °C, and undigested tissue was removed by filtration. Islets were separated from other cells via a Histopaque (Sigma) gradient. Islets were allowed to rest overnight in RPMI media (Sigma) with 11 mM glucose. Ten islets were isolated per well and incubated in the indicated glucose and amino acid concentrations for 30 min. Secreted insulin (Mercodia) and glucagon (Mercodia) were measured by ELISA and normalized to cellular DNA.

Statistical Analysis. Data are represented as mean ± SEM. Statistical analysis was performed using GraphPad Prism. Significance was determined by Student's *t* tests or ANOVA with Tukey's multiple-comparisons test where appropriate. A P value < 0.05 was considered statistically significant.

Data Availability. All data are included in the manuscript and *SI Appendix*.

ACKNOWLEDGMENTS. This work was supported by the Novo Nordisk Foundation Center for Basic Metabolic Research, which is an independent research center at the University of Copenhagen partially funded by an unrestricted donation from the Novo Nordisk Foundation (https://cbmr.ku.dk/) (NNF10CC1016515), as well as the Novo Nordisk Tripartite Immunometabolism Consortium (NNF15CC0018486). The work was partially supported by NIH Grant R01 DK110181 (to R.G.K.) and NIH Grant R01 DA033760 (to B.F.C.).

1. A. Saghatelian *et al.*, Assignment of endogenous substrates to enzymes by global metabolite profiling. *Biochemistry* **43**, 14332–14339 (2004).
2. J. Z. Long, M. LaCava, X. Jin, B. F. Cravatt, An anatomical and temporal portrait of physiological substrates for fatty acid amide hydrolase. *J. Lipid Res.* **52**, 337–344 (2011).
3. J. C. Sipe, J. Waalen, A. Gerber, E. Beutler, Overweight and obesity associated with a missense polymorphism in fatty acid amide hydrolase (FAAH). *Int. J. Obes.* **29**, 755–759 (2005).
4. E. Durand *et al.*, Evaluating the association of *FAAH* common gene variation with childhood, adult severe obesity and type 2 diabetes in the French population. *Obes. Facts* **1**, 305–309 (2008).
5. W. A. Devane *et al.*, Isolation and structure of a brain constituent that binds to the cannabinoid receptor. *Science* **258**, 1946–1949 (1992).
6. R. Mechoulam, L. A. Parker, The endocannabinoid system and the brain. *Annu. Rev. Psychol.* **64**, 21–47 (2013).
7. C. Touriño, F. Oveisi, J. Lockney, D. Piomelli, R. Maldonado, FAAH deficiency promotes energy storage and enhances the motivation for food. *Int. J. Obes.* **34**, 557–568 (2010).
8. J. Fu *et al.*, Oleylethanolamide regulates feeding and body weight through activation of the nuclear receptor PPAR-α. *Nature* **425**, 90–93 (2003).

9. L. A. Tellez *et al*., A gut lipid messenger links excess dietary fat to dopamine deficiency. *Science* **341**, 800–802 (2013).
10. L. M. Lauffer, R. Iakoubov, P. L. Brubaker, GPR119 is essential for oleoylethanolamide-induced glucagon-like peptide-1 secretion from the intestinal enteroendocrine L-cell. *Diabetes* **58**, 1058–1066 (2009).
11. A. S. Husted, M. Trauelsen, O. Rudenko, S. A. Hjorth, T. W. Schwartz, GPCR-mediated signaling of metabolites. *Cell Metab.* **25**, 777–796 (2017).
12. J. L. Blankman, B. F. Cravatt, Chemical probes of endocannabinoid metabolism. *Pharmacol. Rev.* **65**, 849–871 (2013).
13. B. F. Cravatt *et al*., Supersensitivity to anandamide and enhanced endogenous cannabinoid signaling in mice lacking fatty acid amide hydrolase. *Proc. Natl. Acad. Sci. U.S.A.* **98**, 9371–9376 (2001).
14. S. Kathuria *et al*., Modulation of anxiety through blockade of anandamide hydrolysis. *Nat. Med.* **9**, 76–81 (2003).
15. G. Godlewski *et al*., Inhibitor of fatty acid amide hydrolase normalizes cardiovascular function in hypertension without adverse metabolic effects. *Chem. Biol.* **17**, 1256–1266 (2010).
16. K. Ahn *et al*., Mechanistic and pharmacological characterization of PF-04457845: A highly potent and selective fatty acid amide hydrolase inhibitor that reduces inflammatory and noninflammatory pain. *J. Pharmacol. Exp. Ther.* **338**, 114–124 (2011).
17. S. Ghosh *et al*., Full fatty acid amide hydrolase inhibition combined with partial monoacylglycerol lipase inhibition: Augmented and sustained antinociceptive effects with reduced cannabimimetic side effects in mice. *J. Pharmacol. Exp. Ther.* **354**, 111–120 (2015).
18. W. H. Brown *et al*., Fatty acid amide hydrolase ablation promotes ectopic lipid storage and insulin resistance due to centrally mediated hypothyroidism. *Proc. Natl. Acad. Sci. U.S.A.* **109**, 14966–14971 (2012).
19. B. Vaitheesvaran *et al*., Peripheral effects of FAAH deficiency on fuel and energy homeostasis: Role of dysregulated lysine acetylation. *PLoS One* **7**, e33717 (2012).
20. A. Saghatelian, M. K. McKinney, M. Bandell, A. Patapoutian, B. F. Cravatt, A FAAH-regulated class of *N*-acyl taurines that activates TRP ion channels. *Biochemistry* **45**, 9007–9015 (2006).
21. M. Aichler *et al*., *N*-acyl taurines and acylcarnitines cause an imbalance in insulin synthesis and secretion provoking β cell dysfunction in type 2 diabetes. *Cell Metab.* **25**, 1334–1347.e4 (2017).
22. O. Sasso *et al*., Endogenous *N*-acyl taurines regulate skin wound healing. *Proc. Natl. Acad. Sci. U.S.A.* **113**, E4397–E4406 (2016).
23. S.-J. Reilly *et al*., A peroxisomal acyltransferase in mouse identifies a novel pathway for taurine conjugation of fatty acids. *FASEB J.* **21**, 99–107 (2007).
24. M. C. Hunt, M. I. Siponen, S. E. H. Alexson, The emerging role of acyl-CoA thioesterases and acyltransferases in regulating peroxisomal lipid metabolism. *Biochim. Biophys. Acta* **1822**, 1397–1410 (2012).
25. D. P. Waluk, K. Vielfort, S. Derakhshan, H. Aro, M. C. Hunt, *N*-acyl taurines trigger insulin secretion by increasing calcium flux in pancreatic β-cells. *Biochem. Biophys. Res. Commun.* **430**, 54–59 (2013).
26. M. K. McKinney, B. F. Cravatt, Structure-based design of a FAAH variant that discriminates between the *N*-acyl ethanolamine and taurine families of signaling lipids. *Biochemistry* **45**, 9016–9022 (2006).
27. G. Balsevich *et al*., Role for fatty acid amide hydrolase (FAAH) in the leptin-mediated effects on feeding and energy balance. *Proc. Natl. Acad. Sci. U.S.A.* **115**, 7605–7610 (2018).
28. J. Tam *et al*., Peripheral cannabinoid-1 receptor inverse agonism reduces obesity by reversing leptin resistance. *Cell Metab.* **16**, 167–179 (2012).
29. K. Mortensen, L. L. Christensen, J. J. Holst, C. Orskov, GLP-1 and GIP are colocalized in a subset of endocrine cells in the small intestine. *Regul. Pept.* **114**, 189–196 (2003).
30. M. A. Nauck *et al*., Effects of glucagon-like peptide 1 on counterregulatory hormone responses, cognitive functions, and insulin secretion during hyperinsulinemic, stepped hypoglycemic clamp experiments in healthy volunteers. *J. Clin. Endocrinol. Metab.* **87**, 1239–1246 (2002).
31. B. L. Panaro *et al*., β-cell inactivation of Gpr119 unmasks incretin dependence of GPR119-mediated glucoregulation. *Diabetes* **66**, 1626–1635 (2017).
32. A. E. Adriaenssens *et al*., Transcriptomic profiling of pancreatic alpha, beta and delta cell populations identifies delta cells as a principal target for ghrelin in mouse islets. *Diabetologia* **59**, 2156–2165 (2016).
33. N. X. Li *et al*., GPR119 agonism increases glucagon secretion during insulin-induced hypoglycemia. *Diabetes* **67**, 1401–1413 (2018).
34. M. M. Yore *et al*., Discovery of a class of endogenous mammalian lipids with anti-diabetic and anti-inflammatory effects. *Cell* **159**, 318–332 (2014).
35. I. Syed *et al*., Palmitic acid hydroxystearic acids activate GPR40, which is involved in their beneficial effects on glucose homeostasis. *Cell Metab.* **27**, 419–427.e4 (2018).
36. J. Z. Long *et al*., The secreted enzyme PM20D1 regulates lipidated amino acid uncouplers of mitochondria. *Cell* **166**, 424–435 (2016).
37. L. J. Cohen *et al*., Commensal bacteria make GPCR ligands that mimic human signalling molecules. *Nature* **549**, 48–53 (2017).
38. Å. Segerstolpe *et al*., Single-cell transcriptome profiling of human pancreatic islets in health and type 2 diabetes. *Cell Metab.* **24**, 593–607 (2016).
39. S. Chen *et al*., Simultaneous extraction of metabolome and lipidome with methyl *tert*-butyl ether from a single small tissue sample for ultra-high performance liquid chromatography/mass spectrometry. *J. Chromatogr. A* **1298**, 9–16 (2013).
40. H. Gowda *et al*., Interactive XCMS Online: Simplifying advanced metabolomic data processing and subsequent statistical analyses. *Anal. Chem.* **86**, 6931–6939 (2014).
41. J. Xia, I. V. Sinelnikov, B. Han, D. S. Wishart, MetaboAnalyst 3.0—Making metabolomics more meaningful. *Nucleic Acids Res.* **43**, W251–W257 (2015).
42. N. Petersen *et al*., Inhibiting RHOA signaling in mice increases glucose tolerance and numbers of enteroendocrine and other secretory cells in the intestine. *Gastroenterology* **155**, 1164–1176.e2 (2018).
43. T. Sato, H. Clevers, "Primary mouse small intestinal epithelial cell cultures" in *Methods in Molecular Biology*, S. H. Randell, M. L. Fulcher, Eds. (Humana, ed. 2, 2012), pp. 319–328.
44. R. J. Perry *et al*., Dehydration and insulinopenia are necessary and sufficient for euglycemic ketoacidosis in SGLT2 inhibitor-treated rats. *Nat. Commun.* **10**, 548 (2019).
45. G. L. Szot, P. Koudria, J. A. Bluestone, Murine pancreatic islet isolation. *J. Vis. Exp.* 255 (2007).